4B.1 EFFECTS OF TOPOGRAPHY ON TORNADO DYNAMICS: A SIMULATION STUDY

D. C. Lewellen*
West Virginia University, Morgantown, WV.

1 INTRODUCTION

The properties of the near-surface inflow are known to be a critical factor in determining tornado structure and intensity (see e.g., Lewellen and Lewellen (2007a)), so it is natural to expect that topography might significantly impact tornado behavior near the surface. Tornado damage surveys over nontrivial terrain seem to support this general conclusion. For example Forbes (1998) in his study of damage tracks in the May 31, 1985 tornado outbreak in western Pennsylvania (to our knowledge the most extensive field survey of potential topographic effects) highlighted four phenomena he attributed to topographic influence:

- "The damage swaths of supercell tornadoes have frequently been observed to contract in width and intensify on the downward slopes, where vortex stretching appears to occur."
- "Sometimes a very intense swirl occurs at a spot on the downhill slope or at the base of the mountain."
- "On the uphill slope, tornado intensity is usually weakened."
- "Often the intense tornado core re-emerges at the next hilltop plateau. In the process of reorganizing during its uphill climb, the tornado often takes the form of separate, converging swaths. These sometimes appear to be suction vortices of a weak tornado circulation or even separate tornadoes beneath the mesocyclone.

Given the number of factors involved and limited information available in individual cases, however, observations have not allowed systematic determination of the physical processes involved. In this work we use simulated tornadoes passing over idealized topographic elements to analyze some of the mechanisms by which topography can affect tornado behavior.

*Corresponding author address: D. C. Lewellen, MAE Dept. PO Box 6106, WVU, Morgantown, WV, 26506-6106; e-mail: dclewellen@mail.wvu.edu.

2 APPROACH

In contrast with field observations, numerical simulations allow controlled variations of potentially important parameters, treatment of simplified conditions and access to full velocity fields. For this we use a high-resolution large-eddy-simulation (LES) model that we have employed extensively in previous work. For the cases considered here a limited volume ($2\times2\times2$ km^3) moving with the tornado is employed, with different choices of steady converging swirling inflows (rotating cyclonically) applied at the boundaries to produce different types of turbulent vortices within. Details of the model and simulation procedures may be found in Lewellen et al. (2008) and references therein.

The present study requires in addition a means of incorporating surface topography. Conforming the grid mesh to the surface boundary would require significant changes in the LES model components as well as numerically costly mesh regeneration and field interpolations at each timestep (for the desired simulations following a translating tornado). Instead we employ the "Immersed Boundary" method (see e.g. Mittal and Iaccarino (2005) for a general review and Lundquist et al. (2010) for a 2D implementation for atmospheric simulations over complex terrain). Essentially the flow is still solved on a simple Cartesian grid that includes points interior to the desired solid topography, but additional forcing terms are included to implement the flow boundary conditions implicitly at the immersed surface. This is relatively straightforward for low Reynolds number applications where a simple zero velocity condition at the surface can be imposed, but is more challenging for a high Reynolds number LES with parameterized surface conditions. Accordingly an implementation was developed specifically for this project, compatible with features of the existing 3D code that include an aerodynamic surface roughness condition (i.e., a turbulent log-layer), a TKE based subgrid model, staggered grids used for different field variables, and a direct incompressible pressure solver. Accomplishing this without effectively sacrificing grid resolution near the immersed boundary required the development of novel schemes for setting field variables internal to the boundary. Testing and trouble-shooting of different code elements were performed using idealized simulation cases (e.g., flow over a tilted flat plane) as well as full tornado simulations. A more detailed description is planned elsewhere. The resulting implementation of topography proves numerically very efficient, adding little computational overhead since the added computations, while complex, are essentially restricted to a 2D subspace of the domain.

For the current study a large set of simulations were performed (over 250 to date) varying initial tornado swirl ratio, size, and translation speed, and topography shape (ridges, knolls, valleys, ridge pairs, ridges with gaps, etc.), height, length, width, orientation angle and surface roughness. The finest grid resolution in each case was 5 m or less. Only modest-scale localized topographic elements have been considered (as in fig. 1), consistent with the limited domain tornado simulations performed; the potential effects of larger-scale topography on the parent mesocyclone or supercell are not considered. In the simulation frame the topographic feature moves steadily through the domain at the imposed tornado translation speed while the domain inflow conditions driving the tornado are held fixed in time.

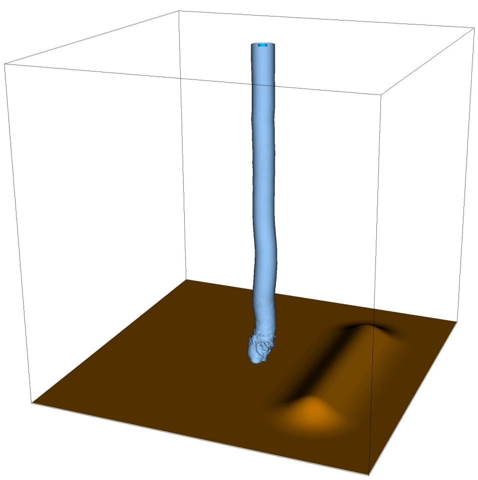

Figure 1: Sample simulation configuration showing $(2\ \text{km})^3$ volume centered around the tornado (indicated by an isosurface of perturbation pressure) with a localized 100 m tall ridge within that moves underneath the tornado in time.

3 TOPOGRAPHIC EFFECTS

Figure 2 shows a sample surface track from the simulation set. The inflow conditions into the simulation domain are held fixed, so in the absence of topography the track would be straight and the central intensity quasi-steady, modulated only by turbulent fluctuations in the tornado corner flow. The large deviations seen in the figure in surface track direction, width and intensity are all direct effects of the topography. Figure 3 gives another view of the same case, highlighting deviations in the time development not apparent from the surface track alone: after an initial deflection the vortex near the surface accelerates up the slope of the first knoll, stays nearly pinned on the back side for an extended time, and then abruptly jumps across the gap to the top of the second knoll. This example is illustrative of the results from the full simulation set. A rich variety

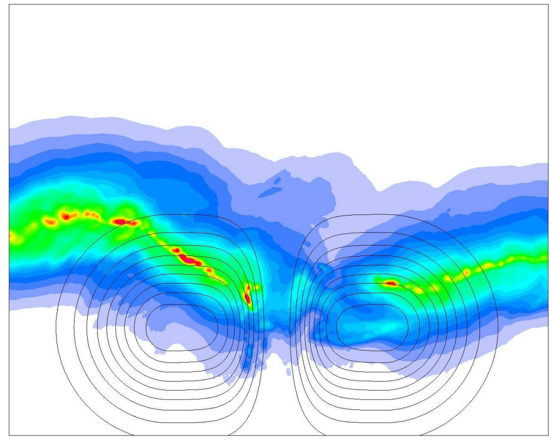

Figure 2: 1 km long "surface track" of peak pressure drops at 3 m height for an initially medium swirl tornado passing from left to right past 100 m tall twin knolls. The imposed translation velocity is 15 m/s, the surface roughness length $z_0 = 20$ cm, and the topographic contour interval shown is 10 m.

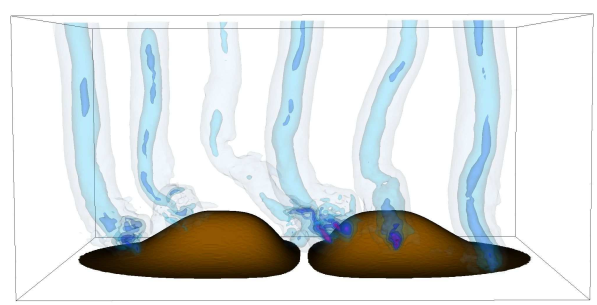

Figure 3: Nested isosurfaces of perturbation pressure drop at six evenly spaced times for the case of fig. 2 (progressing from right to left here, reversed from fig. 2).

of changes in tornado path, intensity, and structure due to interaction with the terrain have been found. The effects vary strongly with choice of tornado type, scale and translation speed, as well as topography shape, scale, alignment and surface roughness. The simulated vortices are sometimes deflected by slopes, sometimes attracted to slopes, sometimes stalled for a time over topographic features, sometimes detached from the surface. The vortices sometimes weaken, sometimes strengthen, heading either up or down slopes, often exhibiting large changes in corner-flow structure during their evolution. Some of the more important dynamical elements involved in the topographic effects are considered now in turn using idealized simulation conditions to assist in isolating different effects.

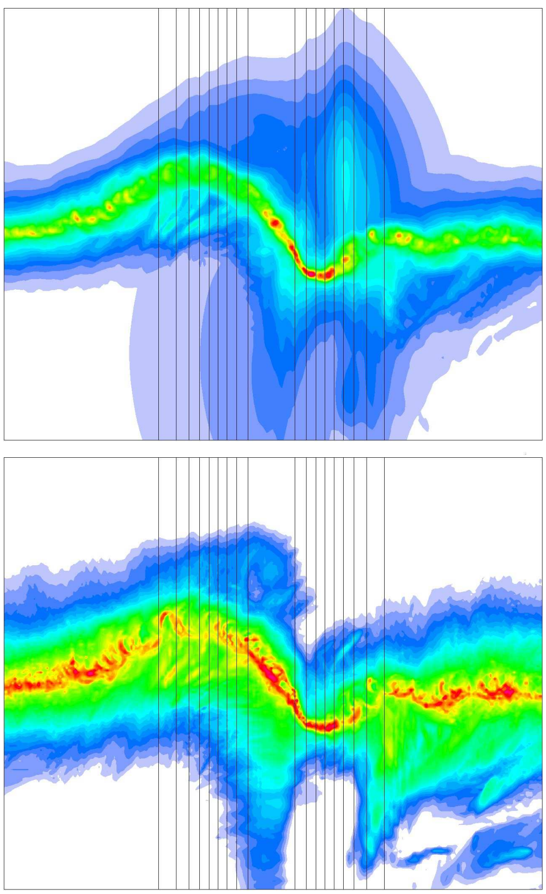

Figure 4: 1 km long surface track of peak pressure drop (top) and peak wind speed (bottom) encountered at 3 m height for a simulated medium swirl tornado moving left to right at 15 m/s across a 100 m tall ridge. The surface roughness length is $z_0 =$ 2 cm, and the topographic contour interval shown is 10 m.

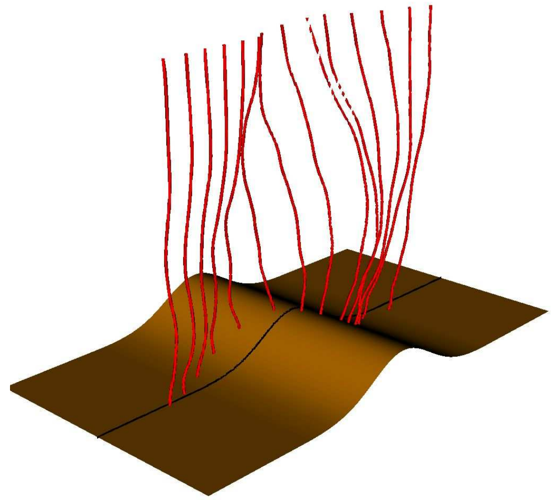

Figure 5: Superposition of the central vortex axis at equally spaced points in time for the case of fig. 4 (progressing left to right). The black line indicates the straight surface track that would have occurred in the absence of any topographic deflection.

3.1 Tornado path deviations

Figures 4 and 5 illustrate the surface track for a basic case of a tornado approaching normal to a ridge. At least to first order the topographically induced path deviations in this and other cases can be understood in the approximation of the tornado as an inviscid line vortex (with cyclonic rotation) in an otherwise irrotational flow. Three main elements are involved:

1. A line vortex angled relative to a solid surface induces a translation velocity directed normal to the plane containing the line vortex and its mirror image across the surface.

2. Different segments of a curved vortex induce translation velocities on other segments, given by the Biot-Savart law.

3. The axis of a line vortex just above a solid surface tends to align perpendicular to that surface.

Element (1) can be understood approximately by considering the "method of images" for imposing boundary conditions at a solid surface: an "image vortex" segment below the surface is angled relative to the vortex segment above the surface, inducing a velocity upon it in analogous fashion to (2). Element (3) is a consequence of the normal pressure gradient at the surface tending to zero in the boundary layer approximation of the Navier-Stokes equations.

As the vortex in fig. 5 initially approaches the ridge, the image vortex below the ridge induces it to move to

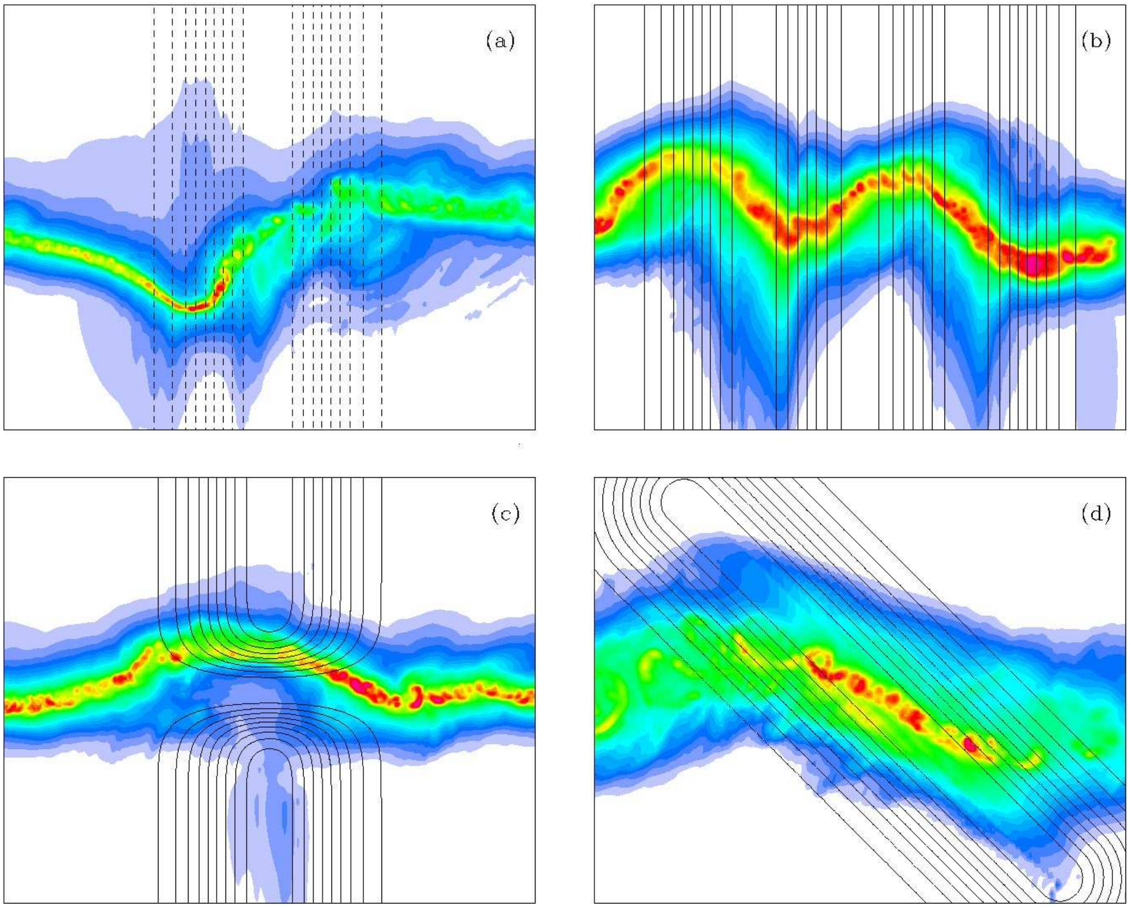

Figure 6: Surface tracks of peak pressure drop at 3 m height for simulated tornadoes crossing: (a) a valley, (b) a double ridge, (c) a gapped ridge, and (d) a slanted ridge. (a)-(c) were initially medium swirl vortices and the roughness length was $z_0 = 2$ cm; (d) was initially a high-swirl vortex and the roughness length was $z_0 = 20$ cm. In each case the maximum topography amplitude was 100 m, the contour interval 10 m, the translation velocity 15 m/s, and the track progresses left to right.

the left. As it climbs the ridge the lower vortex aligns perpendicular to the hillside; the resulting tilt relative to the surface preceding the ridge now induces a motion back to the right. Meanwhile the curvature in the vortex arising from the initial leftward deflection at the surface induces a velocity accelerating the vortex up the ridge (evident in the increased axis spacing on the front side of the ridge in fig. 5); on the backside of the ridge the vortex curvature is such to slow the vortex descent (evident by the bunching of the axis spacing near the surface on the backside of the ridge). There are also higher order corrections altering the tornado path: effects of vorticity not concentrated in the tornado core, effects of surface roughness, and both near-field and far-field effects of the topography on the near-surface inflow and hence positioning of the vortex at the surface.

All of the highlighted effects interact with each other and integrate over time to produce non-trivial path deflections over different topographies. Figure 6 provides some examples, including a rightward deflection entering a valley, double deflections over a twin ridge, the active avoidance of a gap in a ridge and a sometime tendency to travel along ridge tops.

3.2 Tornado intensity and structure

The examples in fig. 6 also illustrate many of the features quoted above from Forbes (1998), particularly the tendency for vortex intensification on uphill slopes and weakening on downhill slopes, and in fig. 6d the tendency toward vortex reorganization on the uphill slope with an intense track appearing at ridge top. The ability to perform idealized parameter variations in the simulations and study the full velocity fields allows the mechanisms responsible for the topographic effects on tornado intensity and structure to be identified. If the tornado were a purely swirling flow, then the dominant available mechanisms would be vortex compression on uphill slopes and stretching on downhill slopes. The frequent tendency seen in tornado tracks for upslope weakening and downslope strengthening is often attributed to this mechanism, but this does not explain the frequent intensification at ridge tops, the apparent changes in tornado structure, or (in the simulations at least) the occasional appearance of upslope strengthening and/or downslope weakening. Tornadoes are not purely swirling flows, particularly near the surface. A detailed examination of evolving wind fields in the simulations shows that the dominant mechanisms by which topography affects vortex intensity and structure are in fact via changes in near-surface inflow with its resulting affects on corner flow swirl ratio, S_c.* There are

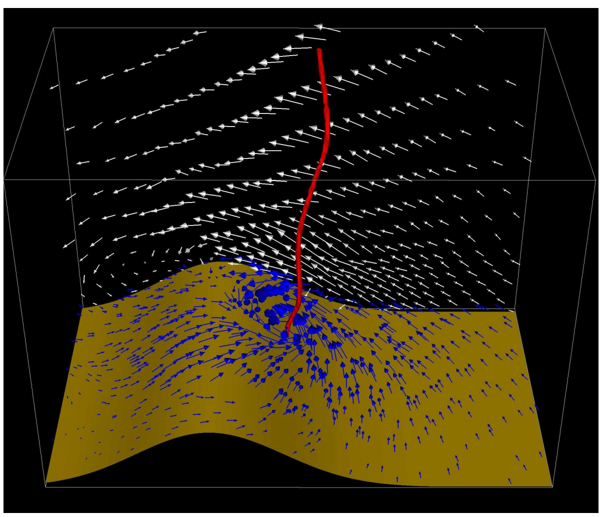

Figure 7: Sample velocity vectors 10 m above the surface (blue) and on a selected vertical plane (white) for a tornado heading upslope (moving right to left); vectors are given in a reference frame with the ground at rest. The red line represents the mean vortex core position at the time. The simulation case is that of fig. 4.

two primary competing effects (c.f., fig. 7). Climbing up a hillside the near-surface swirl flow component can be deflected back toward the vortex by the hill, effectively increasing the near-surface swirl component and thus S_c. More dramatically, as the vortex approaches a ridge top, a flow separation from the ridge top (c.f., the white vectors in fig. 7) leads to a pool of low-swirl fluid on the backside of the ridge that can be drawn in along the surface into the vortex corner flow, effectively lowering its S_c. The relative weight of these two components and net effect on intensification and structure depends on many factors including initial S_c, translation velocity, z_0 and topography. Generally a decrease in S_c will increase vortex intensity if S_c is above the critical low-swirl peak and lower intensity otherwise (Lewellen et al., 2000). The degree of flow separation at ridge top will be increased by increases in z_0, translation velocity (at least on one side of the vortex), overall velocity scale, and steepness of the ridge. There are also additional effects that can influence near-surface wind intensity, such as simple Bernoulli speed-up of velocities across a ridge top, near-surface weakening from transient flow separation on lee slopes, and transient intensification of selected secondary vortices in some high-swirl tornadoes due to topography induced asymmetries in near-surface flow.

Consider as an example the case of fig. 4, for which an examination of the full velocity fields shows the following. As the vortex initially climbs the ridge a combination of vortex compression and deflection of the near-surface flow into the swirl direction by the hillside effectively increases the corner flow swirl ratio from medium to higher swirl, weakening it. As the ridge top is approached, however, the low-swirl flow from the flow separation over the ridge leads to lowering S_c and intensification. Once descended down the rear side of the ridge far enough this source is lost and S_c rises again.

Figure 8 illustrates how sensitive these dynamical mechanisms can be to changes in conditions. It differs from the case of fig. 4 only by having a greater surface roughness. This lowers the initial S_c (by increasing the near-surface low-swirl flow component) and also increases the degree of flow separation across the ridge top. The basic mechanisms at work are analogous to those in the case of fig. 4, but the shift in where it lies in parameter space leads to a large difference in the surface tracks. This case provides an example (one of several encountered in the simulation set) of the occurrence of a strong "swirl spot" located on or after a downhill slope, as noted in Forbes (1998). An examination of the full velocity fields from the simulation clarifies the dynamics at work, as partly illustrated here in fig. 9. The increased low-swirl fluid arising from the flow separation at ridge top now drives the vortex S_c (already somewhat reduced initially) first to a one-celled low-swirl corner flow and then further to very low swirl, where the core is flooded with low-swirl flow, weakening it and raising the point of lowest pressure drop aloft (for the vortex just past the ridge top in fig. 9). Further down the backside of the ridge, however, this source of low-swirl flow is strongly re-

*The reader is referred to Lewellen et al. (2000) for definition and further discussion of S_c.

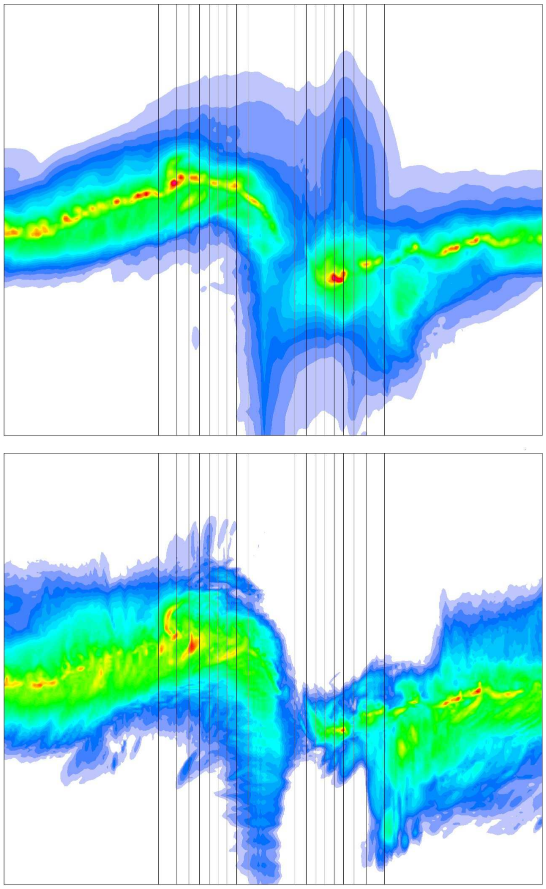

Figure 8: As in fig. 4 but with $z_0 = 20$ cm.

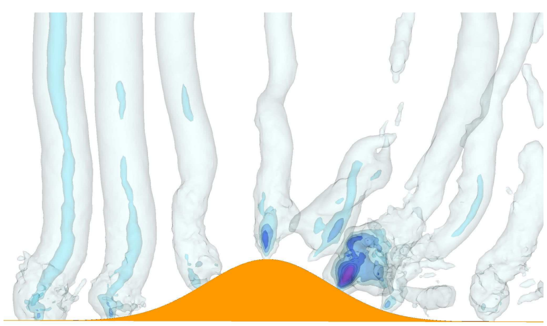

Figure 9: Superposition of nested perturbation pressure isosurface at equally spaced points in time (every 7.5 s) for the case of fig. 8 (progressing left to right).

duced. This provides the ingredients, on the tornado scale, for the phenomenon of "corner flow collapse" (Lewellen and Lewellen, 2007a,b), and a detailed examination confirms that this is the origin of the strong "swirl spot" in the simulation. The enhanced core updraft continues to remove low-swirl fluid from the corner flow, but the near-surface source of low-swirl fluid to replace it is lost; higher-swirl flow is drawn in in its stead leading to the dramatic near-surface intensification seen in fig. 9.[†]. The intensification is short lived since the low pressure produced eventually drives a compensating central downdraft that re-expands and thereby weakens the near-surface core.

The main topographically influenced ingredients altering tornado structure that are seen in the simulations are the same as those affecting tornado intensity, and again arise mainly through effective changes in corner flow swirl ratio as already noted. Some other features occasionally encountered within the simulation set were strong curvature of the vortex axis induced by the local slope, strong transient rotors aloft above a lee slope, asymmetries leading to strong transient secondary vortices, secondary vortices following along ridge tops, and stalling or jumping of the point of contact of the vortex on the surface.

4 CONCLUSIONS AND WORK IN PROGRESS

A set of simulations of tornadoes interacting with topography on the tornado scale have shown that even modest amplitude topography can lead to significant changes in tornado strength, structure and path. Multiple, sometimes competing, effects lead to a great variety of behaviors, with the largest influences generally from topographically induced changes in the near-surface inflow to the tornado.

Several extensions of the work are in progress. The parameter space relevant to topographic effects on tornadoes is large, so despite the large number of simulations performed to date, many important regimes remain to be explored. In addition the implementation of the immersed boundary method within the LES model is being extended to allow the direct simulation of tornado pressure and debris forcing on simple building structures for a variety of realistic wind fields, and to address the potential importance to tornado dynamics of treating individual surface roughness elements rather than simply employing a surface roughness length approximation. Finally, given the sensitivity of near-surface tornado intensity to topography, it is worth considering whether, in a statistical sense for a variety of tornado types, some small-scale topographic configurations might effectively reduce tornado damage potential for some limited areas.

[†]Note that the one order of magnitude increase in near-surface pressure drop relative to peak pressure drops aloft encountered here, while dramatic, is relatively modest to what can be achieved in some corner flow collapse events.

5 ACKNOWLEDGMENTS

This material is based upon work supported by the National Science Foundation, under Grant 1013154.

References

Forbes, G. S., 1998: Topographic influences on tornadoes in Pennsylvania. *Preprints, 19th Conference on Severe Local Storms*, Amer. Meteor. Soc., Mineapolis, MN, 269-272.

Lewellen, D. C., B. Gong, and W. S. Lewellen, 2008: Effects of fine-scale debris on near-surface tornado dynamics. *J. Atmos. Sci.*, **65**, 3247–3262.

Lewellen, D. C., and W. S. Lewellen, 2007a: Near-surface intensification of tornado vortices. *J. Atmos. Sci.*, **64**, 2176–2194.

Lewellen, D. C., and W. S. Lewellen, 2007b: Near-surface vortex intensification through corner flow collapse. *J. Atmos. Sci.*, **64**, 2195–2209.

Lewellen, D. C., W. S. Lewellen, and J. Xia, 2000: The influence of a local swirl ratio on tornado intensification near the surface. *J. Atmos. Sci.*, **57**, 527–544.

Lundquist, K. A., F. K. Chow, and J. K. Lundquist, 2010: An immersed boundary method for the weather research and forecasting model. *Mon. Wea. Rev.*, **138**, 796–817.

Mittal, R., and G. Iaccarino, 2005: Immersed boundary methods. *Ann. Rev. Fluid Mech.*, **37**, 239–262.